

# Poly(propyleneimine) Dendrimer-Gold Nanoparticle Modified Exfoliated Graphite Electrode for the Electrochemical Detection of *o*-nitrophenol

Thabile Ndlovu<sup>1\*</sup>, Omotayo A. Arotiba<sup>\*</sup>, Bhekie B. Mamba

Department of Applied Chemistry, University of Johannesburg, PO Box 17011, Doornfontein 2028, Johannesburg, South Africa,

\*E-mail: [oarotiba@uj.ac.za](mailto:oarotiba@uj.ac.za); [thabilenbk@gmail.com](mailto:thabilenbk@gmail.com)

Received: 12 May 2014 / Accepted: 25 September 2014 / Published: 28 October 2014

---

The electrochemical detection of *o*-nitrophenol (*o*-NP) on a poly(propyleneimine) dendrimer-gold nanocomposite modified exfoliated graphite electrode (EG) is presented. The nanocomposite was prepared by a single step electro-co-deposition method using cyclic voltammetry onto a lab fabricated EG electrode. The PPI-AuNP modified EG electrode exhibited an enhanced electro-activity for *o*-NP reduction over both EG electrode and nanocomposite modified glassy carbon electrode. Square wave voltammetric cathodic peak current of *o*-NP was proportional to the *o*-NP concentration between  $3.1 \times 10^{-7} \text{ mol L}^{-1}$  –  $5.0 \times 10^{-5} \text{ mol L}^{-1}$ , with a detection limit of  $3.3 \times 10^{-8} \text{ mol L}^{-1}$ . No interference was observed from other phenolic compounds except nitro containing compounds.

---

**Keywords:** exfoliated graphite electrode, *o*-Nitrophenol, poly(propyleneimine) dendrimer, gold nanoparticle, nanocomposite

## 1. INTRODUCTION

The use of electrochemical techniques for the detection of nitrophenols has resulted in interesting results where low detection limits have been obtained. In most cases, modified electrodes were used to achieve these results. Hutton *et al* used a bismuth film modified glassy carbon electrode (GCE) for the detection of 2-nitrophenol, 4-nitrophenol, and 2,4-dinitrophenol with detection limits of  $0.4 \mu\text{g L}^{-1}$ ,  $1.4 \mu\text{g L}^{-1}$  and  $3.3 \mu\text{g L}^{-1}$  respectively [1].

Carbon based materials are suitable for electrochemical detection of various analytes due to their favourable properties such as good conductivity and resistance to environmental and chemical hazards. The most widely used carbon electrode is the either in its pristine or modified form is the

---

<sup>1</sup> Author's Present Address: Department of Chemistry, University of Swaziland, Private Bag 4, Kwaluseni, Swaziland

glassy carbon electrode (GCE). In the electroanalysis of environmental pollutants, GCE has been employed for both organic and inorganic contaminants. Examples of environmental organic pollutants detected with GCE include bisphenol A [2], chlorophenols [3], atrazine [4] and nitrophenols [1,5].

Glassy carbon is extremely hard and thus difficult to shape and fabricate into an electrode (especially in the laboratory), making its production process expensive [6]. The formation of strong covalent bonds such as C-N on the electrode surface can be a challenge as these are very difficult to break hence making it challenging to regenerate a clean electrode surface. Chemically aggressive cleaning methods may be used to clean the electrode surface but this in turn might damage the electrode surface. These shortcomings necessitate the quest for a wider carbon material range of which exfoliated graphite is an example. Exfoliated graphite (EG) is corrosion resistant, low in cost and is structurally and chemically amenable to modification [7]. The EG electrode surface is also easily renewable by a polishing step owing to its lubricating property.

In our previous study, a GCE was modified with a nano-composite of poly(propyleneimine)-gold (PPI-AuNP) for the detection of *o*-nitrophenol with interesting results [8]. In this work, we report the use of a fabricated exfoliated graphite electrode modified with PPI-AuNP for the detection of the model pollutant, *o*-nitrophenol.

## 2. EXPERIMENTAL

### 2.1. Reagents and Instruments

Generation 2 (G2) poly(propyleneimine) (PPI) dendrimer was purchased from SyMO-Chem, Eindhoven, Netherlands. All other chemicals such as  $\text{HAuCl}_4$ , natural graphite, *o*-nitrophenol,  $\text{K}_3\text{Fe}(\text{CN})_6$ ,  $\text{K}_4\text{Fe}(\text{CN})_6$ ,  $\text{KH}_2\text{PO}_4$ ,  $\text{K}_2\text{HPO}_4$ ,  $\text{HCl}$ ,  $\text{KOH}$  were bought from Sigma Aldrich. All aqueous solutions were prepared with double distilled water. Phosphate buffer solution (0.1 M, PBS) of pH 5 and pH 7 was used for *o*-NP solutions and PPI-AuNP modification, respectively. All electrochemical measurements were done on an Autolab PGSTAT 302N using a three electrode configuration. Working, counter and reference electrodes were GCE and EG, platinum wire and  $\text{Ag}/\text{AgCl}$  (3M  $\text{Cl}^-$ ), respectively. An amplitude of 50 mV and a frequency of 25 Hz were used for square wave voltammetry (SWV).

### 2.2. Electrode preparation

The EG electrode was fabricated as previously reported [9]. Natural graphite (NG) flakes of particle size  $\pm 300 \mu\text{m}$ , were soaked in a mixture of concentrated  $\text{H}_2\text{SO}_4$  and  $\text{HNO}_3$  (3:1, v/v) at room temperature and pressure to form graphite intercalated compound (GIC). The GIC was washed until neutral pH and subjected to thermal shock at  $800^\circ\text{C}$  for about 30 seconds to produce exfoliated graphite (EG). EG was recompressed to form sheets which were cut into 3 mm circular discs which were used to fabricate the EG electrode. A copper wire was used to facilitate conductivity between the

EG discs with conducting silver paint acting as a glue. This was inserted into a glass rode insulated with a non-conducting epoxy resin, leaving the EG pellet as the only exposed conducting surface.

The modification of the EG electrode with PPI-AuNPs was carried by electro-co-deposition. Equal amounts (5 mL) of solutions containing 10 mM Generation 2 (G2) PPI and 5 mM H<sub>AuCl</sub><sub>4</sub> in PBS supporting electrolyte at pH 7 were prepared and mixed. PPI and H<sub>AuCl</sub><sub>4</sub> were electro-co-deposited using cyclic voltammetry (CV) by cycling between the potentials of -350 mV to 1100 mV for 10 cycles [8]. All potentials presented in this work were measured with respect to the Ag/AgCl (3 M KCl) reference electrode.

### 3. RESULTS AND DISCUSSION

#### 3.1. EG electrode characterisation

Exfoliated graphite is prepared by intercalating natural graphite (NG) with bisulphate ions (from concentrated acids to form graphite intercalated compound (GIC). Followed by a sudden and intense temperature increase resulting in the vaporisation and violent expulsion of the bisulphate ions intercalated within the natural graphite lattices, thus expanding the *c*-axis distance [10]. The densities were calculated to be 0.0068, 0.54 g mL<sup>-1</sup> and 0.144 g mL<sup>-1</sup> for EG, NG and GIC, respectively.

The crystallinity of the graphitic material was analysed using Raman spectroscopy. This technique has been shown to be a good tool to evaluate the crystallinity and the defects in sp<sup>2</sup>-hybridised carbon structures. The Raman spectrum of graphite has been reported to show bands at about 1370, 1583, 2400 and 2700 cm<sup>-1</sup>, designated as D, G, D' and G' bands respectively [11].

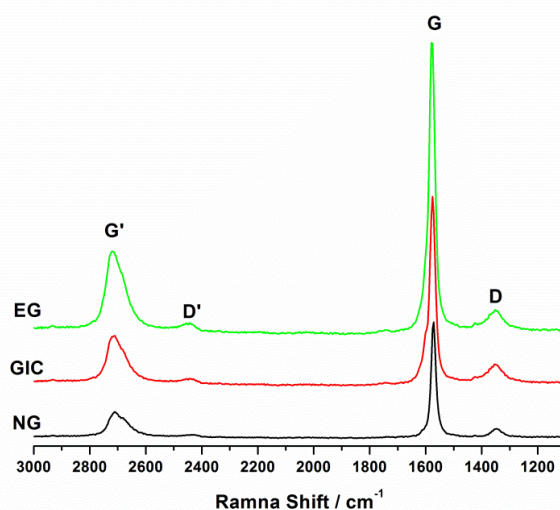


**Figure 1.** Raman spectra of the different graphite materials.

From the Raman spectra of NG, GIC and EG four major peaks were observed at 1358 cm<sup>-1</sup>, 1578 cm<sup>-1</sup>, 2445 cm<sup>-1</sup>, 2724 cm<sup>-1</sup> corresponding to the D, G, D' and G' bands respectively as shown in

Figure 1. The G band is due to the first order scattering process in graphite [12] while the D band is due to the presence of the distributed edge planes [10]. The G' and D' bands originate from a second order process where the D' band is due to the disorder in the c-direction [10,12]. The intercalation and exfoliation of graphite did not have an effect on the crystallinity of the material as the ratio of G and D bands, D/G, (as well as G' and D') were very small.

The EG was recompressed into a pellet and then used to fabricate a 3 mm electrode which was polished on emery paper of different grids before use. This electrode was electrochemically characterised using cyclic voltammetry (CV) in a well known redox probe,  $K_4[Fe(CN)_6]/K_3[Fe(CN)_6]$  (referred to as  $[Fe(CN)_6]^{-2/-3}$ ) and KCl as the supporting electrolyte. The CV obtained from this electrode showed good reversibility which is characteristic of this redox probe as shown in Figure 2a. This was seen as a reversible pair at *ca* 300 mV and 200 mV for the oxidation and reduction peaks, respectively. The same solution of  $[Fe(CN)_6]^{-2/-3}$  solution was used to record the CV using a commercial GCE and the results are shown in Figure 2. Although the GCE gave lower peak separation,  $\Delta E$ , (*ca* 80 mV as compared to *ca* 100 mV for EG), the EG electrode gave higher peak currents for both the redox peaks, a property that is essential for sensors.

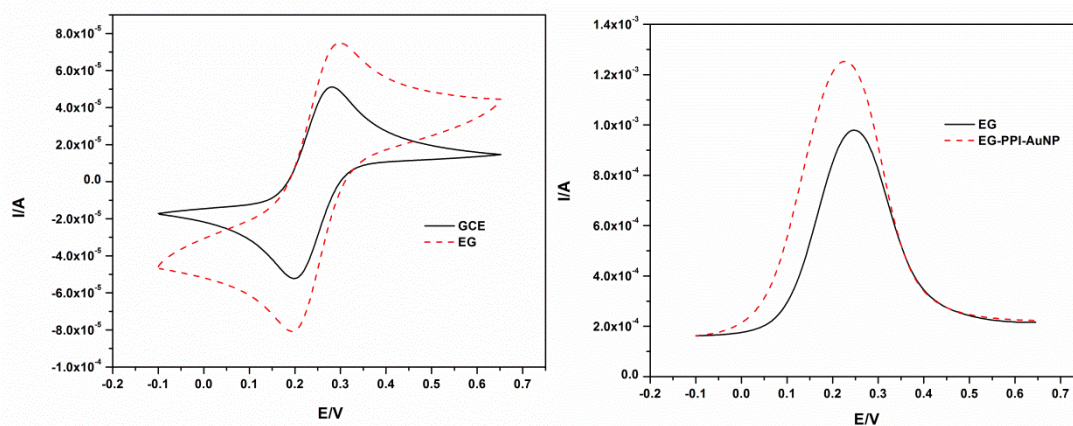


**Figure 2.** a) CVs on 5 mm  $[Fe(CN)_6]^{-2/-3}$  in 0.1 M KCl at a scan rate of 20 mVs<sup>-1</sup> using GCE and EG electrodes b) SWVs of  $[Fe(CN)_6]^{-2/-3}$  in 0.1 M KCl at an amplitude of 50 mV

From the CV results, the electroactive surface areas of 3.95 mm<sup>2</sup> for the EG electrode and 3.23 mm<sup>2</sup> for the GCE were calculated from Randle-Sevcik equation. It was observed that the peak currents of both redox peaks were proportional to the square root of the scan rate (voltammograms not shown) for both EG and GCE. These results indicated that the electrochemical kinetics signified a diffusion-controlled process at the different scan rates which suggest that EG has good electrochemical properties which can allow its use in quantitative analyses. Diffusion-controlled processes are characterised by fast electron transfer at the electrode surface. This implies that the EG electrode also exhibits fast electron transfer kinetics at the electrode surface.

Square wave voltammetry (SWV) was used to record voltammograms in the  $[Fe(CN)_6]^{-2/-3}$  redox probe and the modified electrode showed a *ca* 20% increase in the peak current as shown in

Figure 2b - an enhancement suitable for electroanalytical purposes. In this study, the modified EG electrode was further investigated for possible use in the detection of *o*-nitrophenol.

### 3.2. Electrochemical behaviour of *o*-NP

The electrochemical behaviour of *o*-nitrophenol was first investigated on the EG electrode and the results are shown in Figure 3. Four peaks typical of the electrochemical behaviour of nitrophenols were observed from the CV of *o*-nitrophenol. This electroactivity results from the nitro group ( $-\text{NO}_2$ ) and the hydroxyl group ( $-\text{OH}$ ). When scanning cathodically, the largest peak was observed at *ca*  $-0.586$  V and this was an irreversible peak labelled A in Figure 3 (black line). On the oxidation sweep, there was one anodic irreversible peak (B) at *ca*  $0.185$  V. According to literature, peak A is a result of the reduction of the  $-\text{NO}_2$  group which yields  $-\text{NHOH}$  and this reaction is irreversible [5, 8, 13, 14]. Peak B is due to the oxidation of the hydroxyl group of *o*-nitrophenol. Figure 3 also shows that as the number of scans increases, the peak currents of peaks A and B decreases. The CVs obtained in this experiment were in agreement with most of the electrochemical studies of *o*-nitrophenol [5, 14].

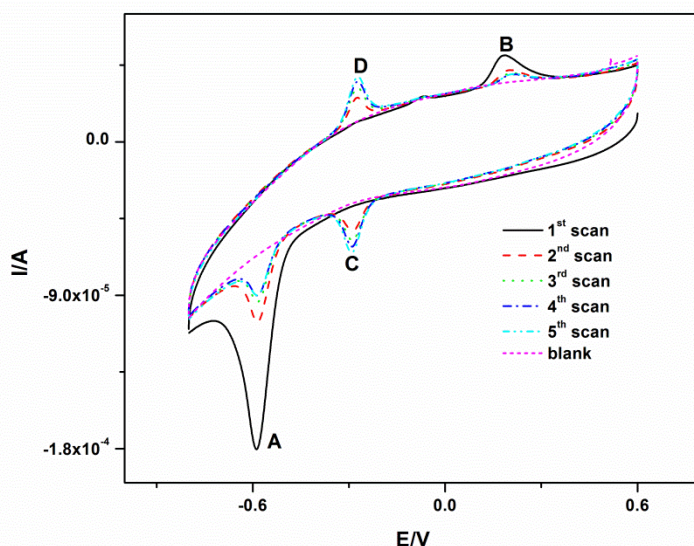
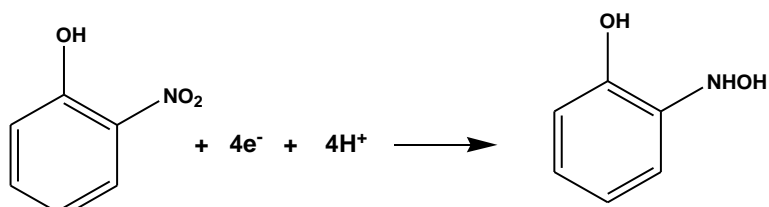
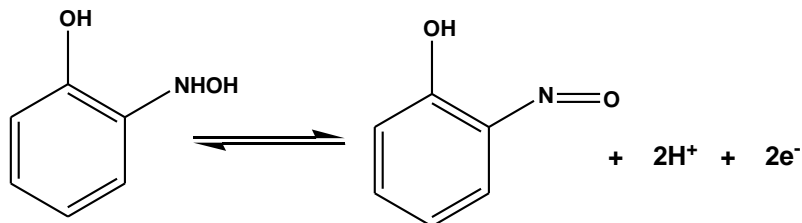


**Figure 3.** CVs showing the electrochemical behaviour of *o*-NP on EG-PPI-AuNP electrode in 0.1 M phosphate buffer at a scan rate of  $50 \text{ mVs}^{-1}$ .

On the second reductive scan (red line), a second cathodic peak (C) was observed at *ca*  $-0.291$  V and an anodic peak (D) at *ca*  $-0.276$  V. These two peaks (C and D) are a reversible couple, and their peak currents kept increasing with increase in scan number. Peaks C and D appear on the second scan because they are new products formed during the reduction of the nitro group as illustrated in eqn 1 and 2. These peaks can only be observed once the  $-\text{NHOH}$  has been formed hence they can only be seen on the second scan.



Eqn 1



Eqn 2

The decrease in A indicated that the products of the irreversible reduction of *o*-nitrophenol remained on or in proximity of the electrode surface and were oxidised on the anodic sweep. This therefore suggests that the amount of pure *o*-nitrophenol at the electrode surface was decreasing with every scan while forming more of the reversible pair products. This was confirmed by stirring the solution for 60 seconds and then running the CV which resulted in comparable peak currents for A for the first CV cycle. According to Zhang *et al*, the decrease of B is attributed to the polymerisation of phenol at the electrode surface [15]. The oxidation of phenol containing compounds is well known and it results in the formation of a polymer which insulates the electrode surface and hence inhibits further phenol oxidation [16]. For peak B, stirring the solution did not improve its peak height due to electrode fouling.

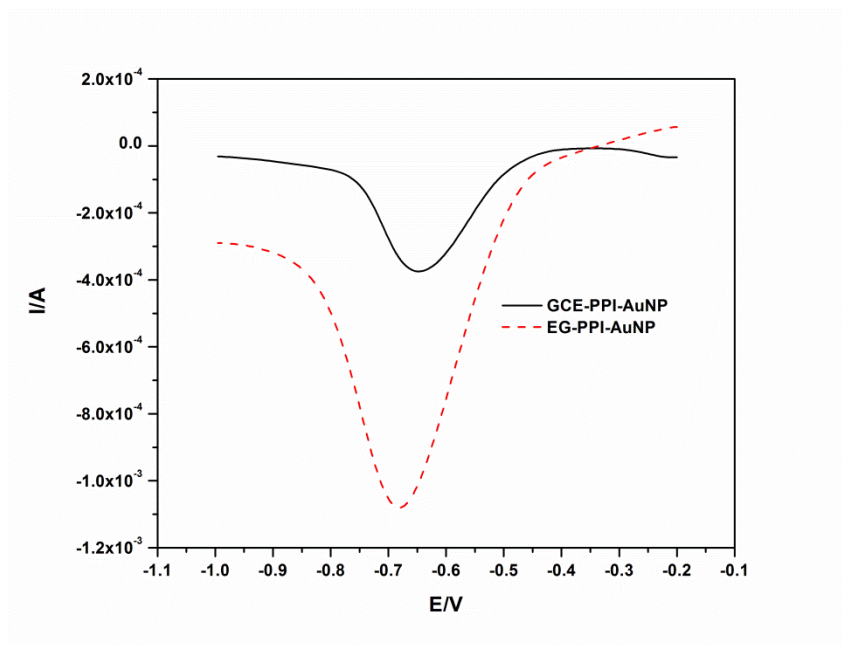


**Figure 4.** A comparison of the SWV of 5 mM *o*-nitrophenol on GCE-PPI-AuNP and EG-PPI-AuNP.

Our earlier study [8], revealed that PPI-AuNP nanocomposite had enhancing and catalytic effects on the reduction of *o*-nitrophenol over bare GCE [8]. This modifier is studied in this on a cheap EG electrode which was fabricated in our lab. This electrode showed better analytical sensitivity as the

peak current observed in 5 mM *o*-nitrophenol was much higher than that observed using the GCE as shown in Figure 4. The EG-PPI-AuNP electrode recorded peak current which was 55% higher than that observed on the GCE-PPI-AuNP electrode. This is not surprising as the EG electrode was shown to possess higher electroactive surface area than the GCE. This high electroactive surface area observed on the bare electrode also results in an even higher surface area on modification, which can be seen as an increase in peak currents when accompanied by the catalytic nature of the nanocomposite. The higher SWV peak current on the EG-PPI-AuNP versus the GCE-PPI-AuNP suggests that a lower detection limit (better sensitivity) can be obtained when using EG-PPI-AuNP.

### 3.3. Effect of pH

The effect of the change in pH on the electrochemical behaviour of *o*-nitrophenol was investigated and peak current was maximum at pH 5 (Figure 5). This result is in line with other results where pH 5 was found to be the best pH for the detection of nitrophenols [17]. The pH also had an evident effect on the peak potential which shifted to more negative potentials with an increase in pH. This behaviour suggests that protons intervened in the oxidation process [18]. The pH versus peak potential plot (Figure 5) was a linear graph with a regression equation:  $E_{pa} = -0.050\text{pH} - 0.268$  with an R value of 0.9900. This implies that the protons of the electrochemical reduction of *o*-nitrophenol do not change over the studied pH range.

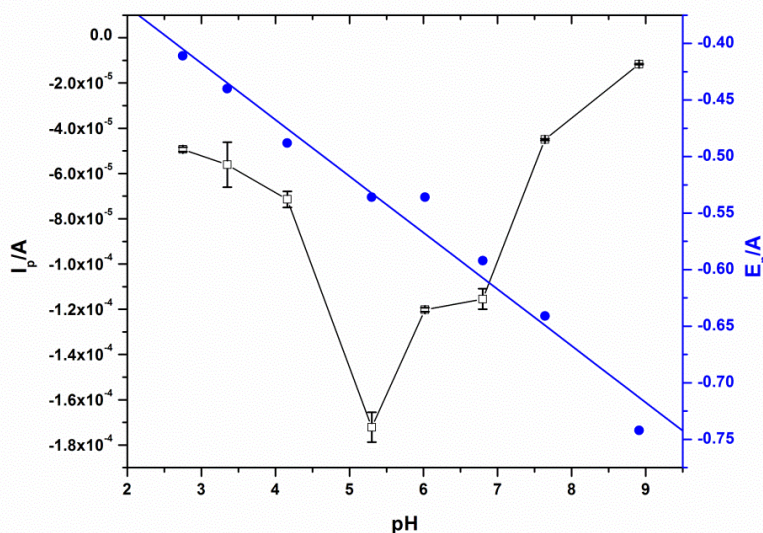


**Figure 5.** Effect of pH on the peak current and peak potential when using the EG-PPI-AuNP electrode in a  $30 \times 10^{-5}$  M solution of *o*-nitrophenol.

### 3.4. Detection of *o*-nitrophenol

The peak current increased with an increase in *o*-nitrophenol concentration. A calibration plot for *o*-nitrophenol concentration range of  $3.1 \times 10^{-7}$  mol L<sup>-1</sup> to  $5.0 \times 10^{-5}$  mol L<sup>-1</sup> on the EG-PPI-AuNP electrode is shown in Figure 6. It was observed that there was a linear relationship between

concentration and the peak current with a linear regression equation of  $y = -3.3 x - 6.65 \times 10^{-5}$  and  $R = 0.998$ .

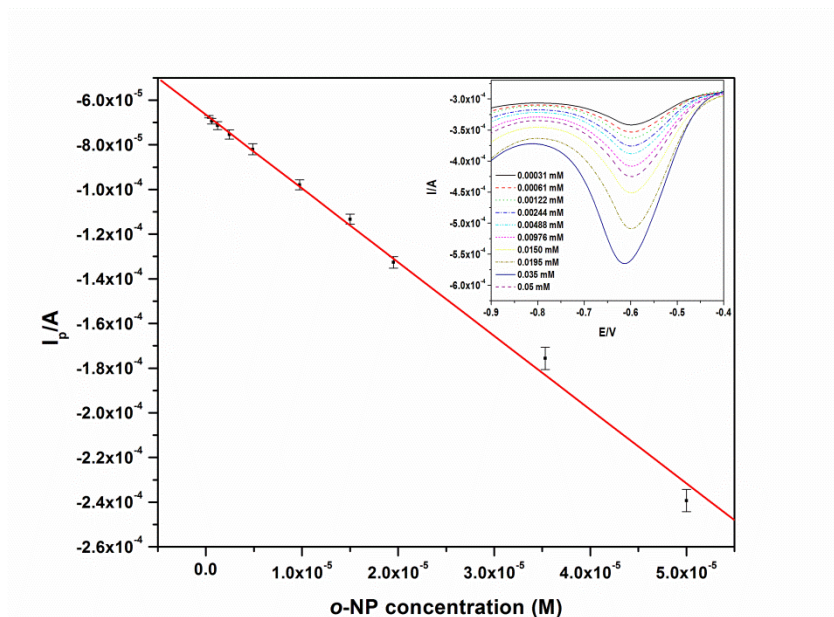


**Figure 6.** Calibration plot for the detection of o-NP (Inset: SWV for different concentration of o-NP on EG-PPI-AuNP in 0.1 mol L<sup>-1</sup> PBS).

The limit of detection was calculated to be  $3.3 \times 10^{-8}$  mol L<sup>-1</sup>. This value is one order of magnitude lower than that obtained on the GCE modified with the same nano-composite [8]. This improved result implies that the EG electrode can be used to detect lower concentrations of o-nitrophenol in lieu of GCE. The detection limit obtained in this study is comparable to those found from other studies using other electrodes as summarised in Table 1.

**Table 1.** Summary of detection limit obtained from other electrochemical sensors

Electrode	Modifier	Detection limit	Reference
TiO <sub>2</sub> nanotube arrays	Au-modified	90 μM for o-NP	[19]
Carbon paste electrode	Hydroxyapatite	8 nM for p-NP	[20]
silver solid amalgam electrode	Mercury meniscus	20 nM for o-NP	[21]
GCE	PPI-AuNP	0.45 μM for o-NP	[8]
diamond electrode	Boron-doped	2.8 μM for p-NP	[22]
Carbon Paste Electrodes	Hexagonal mesoporous Silica	66.7 nM for o-NP	[17]
Exfoliated graphite	PPI-AuNP	33 nM for o-NP	This work

The experiment was repeated five times and the relative standard deviation (RSD) for the peak current of 5 SWVs (for example, 0.015 mM *o*-nitrophenol) was evaluated to be 2.77%, and this revealed that this method has good reproducibility. The results were repeatable even when the electrode was used several days after modification with low RSD suggesting good stability for the electrode.

### 3.5. Interference studies

The current signal for the detection of *o*-nitrophenol can be enhanced or reduced by the presence of other organic compounds such as phenolics and other nitro-containing compounds. For this reason, interference studies were performed in 0.015 mM *o*-nitrophenol and the same concentration of interfering compound which included phenol, bisphenol A (BPA), chlorophenol and *p*-nitrophenol.

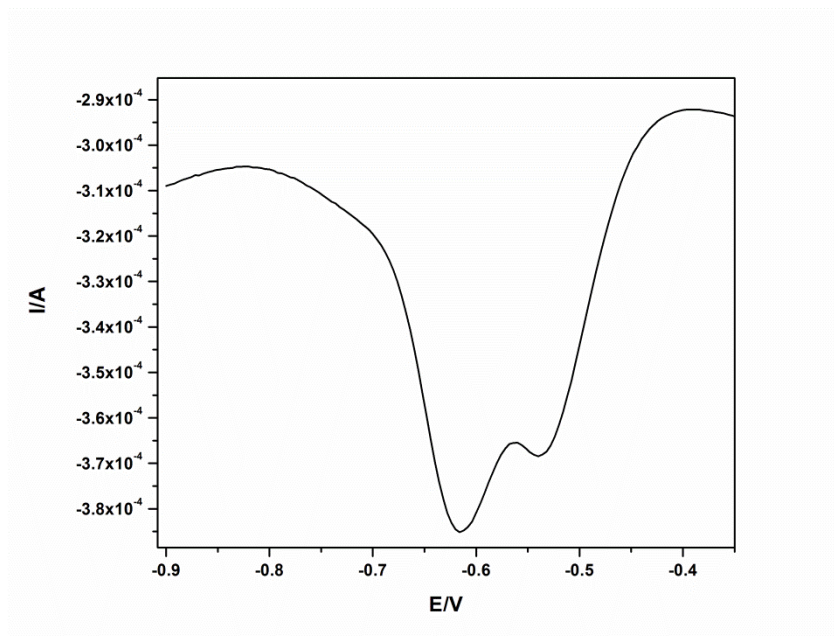


**Figure 7.** SWV taken in the presence of both *o*-nitrophenol and *p*-nitrophenol

There was no interference observed from the phenol, BPA and chlorophenol while there was an overlap of peaks (seen as shoulder) in the presence of *p*-nitrophenols. This is not surprising as these compounds only differ in the positions of the  $-\text{NO}_2$  group. They can undergo the same electrochemical reactions illustrated in eqns 1 and 2. These results imply that if two or more nitro-containing compounds are present in a sample, it can be observed from the SWVs where overlapping peaks can be seen as illustrated in Figure 7. The other phenolic compounds (BPA, phenol and chlorophenol) did not interfere with the reduction signal of *o*-nitrophenol because they do not possess the reducible nitro-group and their hydroxyl group occurs out of the working potentials for *o*-nitrophenol.

#### 4. CONCLUSION

The use of EG for the detection of *o*-nitrophenol has yielded a detection limit lower than that obtained from GCE. This improvement suggests a wider applicability of EG in electroanalysis and also a possible alternative for the conventional glassy carbon electrode. The EG electrode's amenability to modification is a feature that can be further explored and exploited for broader electrochemical applications.

#### ACKNOWLEDGMENTS

The authors would like to thank the Centre for Nanomaterial Science Research, Department of Applied Chemistry University of Johannesburg; Nanotechnology Innovation Centre, South Africa (SA); National Research Foundation (SA); and Council for Scientific and Industrial Research (SA) for funding this project. The support of the Indian Institute of Science is gratefully acknowledged.

#### References

1. E.A. Hutton, B. Ogorevc, M.R. Smyth., *Anal. Electroanal*, 16 (2004) 1621.
2. A. D'Antuono, V. C. Dall'Orto, A. L. Balbo, S. Sobral, I. Rezzano, *J. Agricultural food Chem*, 49 (2001) 1101..
3. S. Zhao, J.H.T., *Anal. Chimica Acta*, 327 (1996) 242.
4. J. Besombes, *Anal. Chimica Acta.*, 311 (1995)255.
5. L. Q. Luo, X. L. Zou, Y. P. Ding, Q. S. Wu., *Sensors. Actuators. Chem*, 135 (2008) 65.
6. P. Monk., John. Wiley. Sons. (2005).
7. A. C. Neto, F. Guinea, N. M. R. Peres, K. S. Novoselov, A. K. Geim, *Rev. Modern Phy*, 81 (2009) 154.
8. T. Ndlovu, O. A. Arotiba, R. W. Krause, B. B. Mamba, *Int. J. Electrochem. Sci.*, 5 (2010) 1186.
9. T. Ndlovu, O. A. Arotiba, , S. Sampath, R. W Krause, , B. B. Mamba., *J. Appl. Electrochem*, 41 (2011) 1396.
10. P. Ramesh, S. Sampath., *Anal. Chem*, 75 (2003) 694
11. G.K. Ramesha, Sampath, Srinivasan., *J. Phy. Chem*, 113 (2009) 7989.
12. L. M. Malard, , M. A. Pimenta, G. Dresselhaus, M. S. Dresselhaus., *Phy. Reports*, 473 (2009) 87.
13. Z. Liu, J. Du, C. Qiu, L.Huang, H.Ma, D. Shen, Y. Ding., *Electrochem. Commun*, 11 (2009) 1368.
14. J. C. Chen, J. L. Shih, C. H. Liu, M. Y. Kuo, J. M. Zen., *Anal. Chem.*, 78 (2006) 3757.
15. D. P. Zhang, W. L Wu, H. Y. Long, Y. C. Liu, Z. S. Yang., *Int. J. Molecular Sci.*, 9 (2008) 326.
16. M.M. Ngundi., *Electrochem. Commun.*, 5 (2003) 67.
17. C. Zhou, Z. Liu, Y. Dong, D. Li., *Electroanalysis*, 21 (2009) 853.
18. X. H. Jia, Q. Li. Zhang, S. F. Wang., *J. Anal. Chem.*, 62 (2007) 269.
19. K.M. Kafi, A. Chen., *Talanta*, 79 (2009) 102.
20. M. A. El Mhammedi, M. Achak, M. Bakasse, A. Chtaini., *J. Hazardous Mater*, 163 (2009) 328.
21. J. Fischer, L. Vanourkova, A. Danhel, V. Vyskocil, K. Cizek, J. Barek, T. Navratil., *Int. J. Electrochem. Sci.*, 2 (2007) 226.
22. V.D. Pedrosa, L. Pedrosa, , L.A. Codognoto, *J. Avaca.*, *Brazilian Chem. Soci.*, 14 (2003) 535.